Article Title:

# Weather Conditions and Warm Air Masses during Active Fire-periods in Boreal Forests

Authors:

**Hiroshi Hayasaka[a*], Koji Yamazaki[b] and Daisuke Naito[c,d]**

*a) Arctic Research Center, Hokkaido University, N21 W11, Kita-ku, Sapporo, Hokkaido, 001-0021, Japan.*

*Tel.: +81-11-706-9073, Fax: +81-11-706-9582*

*Email: hhaya@eng.hokudai.ac.jp*

*b) Faculty of Environmental Earth Science, Hokkaido University, N10 W5, Kita-ku, Sapporo, Hokkaido, 060-0810, Japan.*

*Tel.: +81-11-706-2768, Fax: +81-11-706-4865*

*Email: yamazaki@ees.hokudai.ac.jp*

*c) Center for Southeast Asian Studies, Kyoto University, 46 Yoshida Shimoadachi-cho, Sakyo-ku, Kyoto, 606-8501, Japan*

*Tel.: +81-75-753-9645, Fax: +81-75-753-7350*

*Email: dnaito@gmail.com*

*d) Center for International Forestry Research (CIFOR), P.O. Box 0113 BOCBD, Bogor 16000, Indonesia*

*Tel.: +62-251-8622-622, Fax: +62-251-8622-100*

*Email: dnaito@gmail.com*

•The name and e-mail address of the corresponding author:

Hiroshi Hayasaka

Email: hhaya05@me.com

Arctic Research Center, Hokkaido University, N21 W11, Kita-ku, Sapporo, Hokkaido, 001-0021, Japan.

Tel.: +81-11-706-9073, Fax: +81-11-706-9582

Email: hhaya@eng.hokudai.ac.jp

## ABSTRACT

Weather conditions for concurrent widespread fires in boreal forests were examined by various weather maps and temperature charts. The four study regions in boreal forests are three in East Siberia and one in Alaska. We applied preliminary analysis method for Sakha proposed by the authors to show the effectiveness of our approach. More than 12 very active fire-periods were identified from satellite hotspot data. Analysis results clearly showed fires during all active fire-periods became very active as warm air masses from south approached four study regions. These movements of warm air masses were mainly related to the meandering of large westerlies. To explain the large increase of daily hotspots (fires) during active fire-periods, a preliminary wind analysis was carried out. Strong wind conditions occurred when warm and dry air masses were approaching, stagnating, and passing over Southern Sakha under various weather conditions at lower air. During the top fire-period in Southern Sakha, wind velocity at lower air (925 hPa) changed from about 1 to 8 m/s while number of hotspot increased from around 1000 to 9000.

**Keywords:** Warm Air Mass, Westerlies Meandering, Hotspot, Forest Fire

## 1. Introduction

Boreal forests in eastern Siberia and Alaska are large-scale widespread fire zones (Giglio et al., 2006) and within the region of observed and predicted future accelerated climate change (IPCC, 2016). Forest fires are a natural and inherent element in the functioning of boreal forests (Valendik, 1996, Balzter et al., 2005); however, air temperatures in high latitudes have increased by 0.06 °C per year over the last 30 years, approximately twice as much as global temperatures (IPCC, 2013). Climate-induced fire frequency and burnt areas are increasing in boreal forests, and forest fire frequency has been correlated with air temperature anomalies and drought indices (Field et al., 2015, Ponomarev et al., 2016). Droughts and heat waves associated with a long-term change in background climate can accelerate or intensify forest diseases, insect outbreaks, and fire activity, leading to increased tree mortality (Schaphoff et al., 2015).

In the boreal forests in eastern Siberia, fuel materials are comprised of larch, pine, and spruce, with a ground cover of moss and lichens on permafrost (Onuchin et al., 2007). Fuel materials in Alaska are mainly spruce trees and sphagnum moss (Calef et al., 2005, Hayasaka et al., 2007). These trees have a shallow root system in the upper organic and active layer, and are adapted to permafrost soils. Because of the annual litter fall in eastern Siberia and low decomposition rates of surface fuels (litter fall, moss, etc.), these forests provide organic layers and thus, high fuel levels (Forkel et al., 2012). Increased fire activity has been observed since approximately 1990 for the periods of 1950-2015 in Alaska (Hayasaka, et al., 2016) and 1955-2009 in Sakha (Hayasaka, 2007 and 2011), which have been linked to increasing temperatures (Gillett et al., 2004). In a warming climate, fuel load that has accumulated due to replacement of forest by steppe, together with frequent fire weather, promote high risks of large fires in southern Siberia and central Yakutia. In these areas, wild fires would create habitats for grasslands because the warming and drier climate would no longer be suitable for forests (Tchebakova et al., 2009). Fires with extreme spread and severity could change forests (Kasischke et al., 2010), affecting human values, emitting huge amounts of carbon, and altering the physical properties of the land surface (McGuire et al., 2006). When passing a threshold in frequency or spread, fires could contribute to the dieback of boreal forests as a tipping element in the climate system (Lenton et al., 2008).

Fire size was sensitive to weather in the days to weeks following ignition, particularly the post-ignition timing of precipitation (Abatzoglou and Crystal, 2011). For example, prolonged periods of warm and dry conditions coincident with atmospheric blocking that persisted for several weeks after ignition enabled the growth of large forest fires. Extensive fires in 2004 may have been related to a persistent blocking ridge over Alaska (Bell, 2004; Wendler, et al., 2011). The burnt area in the North American boreal forest was controlled by the frequency of mid-tropospheric blocking highs that caused rapid fuel drying (Fauria and Johnson, 2006, 2008). Furthermore, 500 hPa height anomalies were well correlated with the seasonal burnt area over large regions of Canada and Alaska (Skinner et al., 1999, 2002).

In this study, we focus on weather conditions during active fire-periods in the boreal forests of four study regions: three in eastern Siberia and one in Interior Alaska. Our recent study for Alaska and Southern Sakha has clearly indicated weather conditions in large-scale concurrent widespread fires.

In Alaska (Hayasaka et al., 2016), four of the top seven recent fires occurred related to large Jet stream meandering west of Alaska or Rossby wave breaking (RWB, Tanaka et al., 2004). Preliminary wind analysis using pressure gradient from weather maps carried out to explain wind direction change and wind velocity effect on fire activities. From this report, we have clearly indicated wind condition both at upper (500hPa) and lower (925hPa) air has a significant impact on fires at ground.

Fire activity of the top seven recent fires in Southern Sakha were explained using temperature charts and various weather maps (Hayasaka et al., 2019). Most results were similar with this report. Major differences were: Temperature charts at lower level (925 hPa) were used. Most temperature charts were superimposed on Worldview satellite images with fires. (EOSDIS Worldview, https://worldview.earthdata.nasa.gov/, latest access: July 17, 2019). Preliminary wind analysis using pressure gradient from weather maps or similar analysis in Alaska was carried out to explain large-scale concurrent widespread fires. From this report, we have clearly indicated active fires occurred mainly under stagnating high-pressure systems at upper air (500 hPa). The northward movement of warm air masses from lower latitudes (~40N) toward southern Sakha tended to exacerbate fires mainly due to strong wind conditions at lower air (925hPa) during the fire periods.

Based on these two previous study results for Southern Sakha and Alaska, we try to find common weather conditions available in both eastern Siberia and Alaska. MODIS hotspot data are used to represent the spatiotemporal distribution of fires. To clarify weather conditions, we analyzed atmospheric reanalysis data sets (height, temperature, wind direction and wind velocity) at upper (500 hPa), at middle (850 hPa) and at near surface (925 hPa) levels (Kalnay et al., 1996). Upper-level weather maps were used to evaluate meandering westerlies, and high- and low-pressure systems. Middle-level temperature charts were analyzed to examine northward movement of warm and dry air masses, and their relationship with fire activities.

## 2. Methods and Data

### *2.1 Hotspot (fire) and weather data*

Sixteen years of hotspot (HS) data (2002-2017) detected by moderate resolution imaging spectroradiometer (MODIS) on the Terra and Aqua satellites are used to evaluate fires in boreal forests. MODIS HS data collected during 2002–2017 were obtained from the NASA Fire Information for Resource Management System. (FIRMS; MODIS Collection 6, https://firms.modaps.eosdis.nasa.gov/download/, latest access: April 20, 2019). We use only the spatial and temporal hotspot data in this study. The number of daily hotspots is used to identify fire-periods and the important dates of major hotspot peaks during the fire-periods.

Upper air (500 hPa) and lower air (925 hPa) weather maps, lower air wind maps (925 hPa) and mid air (850 hPa) temperature charts from the NCEP/NCAR 40-year reanalysis data (Kalnay et al., 1996) are analyzed to find common weather conditions and fire-related synoptic-scale circulation patterns, and movement of warm air masses at mid air temperature distributions. Coverage and spatial resolution of the NCEP reanalysis data are: Geographic longitude and latitude: 0.0°E to 358.125°E, -88.542°N to 88.542°N. Spatial resolution: about 2.5° x 2.5°. Period and temporal resolution: 1948/01/01 to now, 6-hourly, daily and monthly.

### *2.2 Study regions in boreal forests*

**Fig. 1** shows four study regions in four rectangles with solid colored line. Three regions in East Siberia and one in Alaska were selected for a comparison of fire activities. For each rectangle, we collected HS data and analyzed them to grasp fire history and active fire-period. We named four target regions: 1. Southern Sakha (SS), 2. Northern Krasnoyarsk (NK), 3. Southern Khabarovsk (SK) and 4. Interior Alaska (IA). **Table 1** shows SS, NK, SK and IA cover regions and their approximate areas. "Area ratio" in Table 1 is introduced to compare the areas at four regions. It shows the area ratio of each region when the area of SS is set to 1. If we need to compare fire activities of the four regions, we can correct the HS numbers of each region for discussion.

Climate type of four study regions (the Köppen climate classification, https://www.thoughtco.com/the-worlds-koppen-climates-4109230 (last access: 5 Jun 2019)), temperature and rainfall in July (Weather underground) measured at Yakutsk (SS), Krasnoyarsk (located at south of NK), Khabarovsk (SK), and Fairbanks (IA) are summarized in **Table 1**. Common climate type of four study regions are “Continental (D)” and “Without dry season (f)”. July is the wettest and the hottest month in most regions (Weather underground). Summer monthly temperature and rainfall trend in Yakutsk and Fairbanks were already reported in our pervious paper (Hayasaka et al., 2007). Daily temperature and rainfall in Yakutsk in 2002 were found in our pervious paper (Hayasaka et al., 2011).

Larch forests, major forest type in East Siberia, distributed three study regions in SS, NK and northern part of SK (Russian vegetation map, Hayasaka et al., 2007 and 2011). Spruce forests are major forest type in Alaska and distributed in central part of IA (Hayasaka et al., 2007).

### *2.3 Top active fire-periods*

We selected top active fire-periods based on previous research by one of the authors (Hayasaka, et al., 2007); that is, consecutive fire days when the number of daily HSs exceeded 300. Active fire-periods are ranked by the number of HSs on HS peak day of each active fire-period. They are named using their ranking in each study region, date, month, year and short name of each region (e.g. “(1)19Aug.’02-SS”, “(2)29Jun.’04-IA”, etc.). In total, 13 very active fire-periods were selected given space limitations of the manuscript: 6 for SS and 5 for IA. Eleven active fire-periods are summarized in

**Table 2**. In **Table 2**, the top six fire-periods in SS are shown in the top of table and the top five fire-periods in IA are listed in the bottom of table. Their numbers of HSs on 11 HS peak days exceed 3,000. On the other hand, there are fewer than 3,000 HSs on HS peak day in NK (2,198) and SK (2,683). We named two active fire-periods, "(1)29Jun.'12-SK" and "(1)22Jul.'16-NK" respectively. From here, we will mainly focus on active fire-periods in two target regions, namely SS and IA.

### *2.4 Fire histories in SS and IA*

Annual fire histories (from 2002 to 2017) in SS and IA are compiled by accumulating the daily number of HSs as shown in **Fig. 2**. **Fig. 2(a)** for SS shows the average number of HSs per year was 25,589. Number of HSs in six years (2002, 2008, 2011, 2012, 2014, and 2017) exceeded the average annual value. From comparison of numbers near each bar graph (largest number of daily HSs in each year), the large number of HSs (exceeding 2,500) was found only in fire years. There is also a very large difference among total number of HSs of each year. The total number of HSs during these years was 554,498. In all, 77.1% of total HSs of 16 years were detected in only five fire years. The largest annual number of HSs was 110,765 in 2002 and the smallest was 570 in 2007. Thus, the largest number of annual HSs was 194 times greater than the smallest (**Fig. 2(a)**); we could call six years (2002, 2008, 2011, 2012, 2014, and 2017) active fire years.

Total number of HSs during the top six fire-periods are shown by a white bar with rank (1~6) in each corresponding bar graph as in **Fig. 2(a)**. Total number of HSs during the top fire-period ("(1)19Aug.'02-SS") in 2002 was 57,033 (**Table 2**), larger than the 46,956 in the top three fire year, 2011. White bar graphs of the top six fire-periods in **Fig. 2(a)** show fires in each year mostly occurred during these fire-periods except in 2011. The total number of HSs of each top five fire-period (**Table 2**) is greater than the largest number of HSs (15,585) in the non-fire year of 2009. Top fire-periods in SK and KK are shown in **Fig. 2(a)** by their corresponding year, 2012 and 2016, respectively. A similar trend is found in IA in **Fig. 2.2**. Detailed trends are already reported in Hayasaka et al., 2007.

Recent fire histories of SS and IA in **Fig. 2** show that 10 fire years in SS and IA took place during different years. The six fire years in SS are 2002, 2008, 2011, 2012, 2014 and 2017. The four fire years in IA are 2004, 2005, 2009 and 2015. In addition, the top fire in SK occurred in 2012 (one of the fire years in SS), while the top fire in NK occurred in 2016 independently from others (**Fig. 2(a)**). **Fig. 2** shows active fire years in NK (92-106 E), SS (120-140 E) and IA (194-220 E, 140-166 W) occurred independently about every two years (1.6=16/10). These fire year trends are discussed using weather conditions in the section 3.2.

## 3. Results and Discussions

### *3.1 Warm and dry air masses of each HS peak day*

Temperature charts of each top HS peak day in study regions are shown in **Figs. 1, 3, 4** and **5**.

A total of 12 temperature charts at mid air (850 hPa) are used to discuss the relationship between HS (fire) and temperature distribution.

**Figs. 1** and **3** show temperature charts of the top five HS peak days in SS, identifying warm and dry air masses over and near SS. They are anvil-shaped contours of temperature 284 K in **Fig. 1** and **Fig. 3(c)**, and three closed circles in **Fig. 3(a)**, **(b)**, **and (d)**. These air masses were released from the north end of a subtropical high-pressure zone at around 40-50 N. Arrowhead lines in **Figs. 1** and **3** show approximate northward routes of each warm air mass; they can be found from corresponding daily temperature charts (not shown due to space limitations). Fires became very active when each warm air mass started to move toward SS. In this manuscript, we refer to these warm and dry air masses as continental temperate (cTe) following the Russian expression (Shahgedanova, 2003). The temperature chart of the top sixth HS peak day is not shown due to space limitations, but cTe is near SS.

**Fig. 4** shows temperature charts of top five HS peak days in IA. In Alaska, most warm and dry air masses moved northward along the Rocky Mountains and reached IA. These movements occurred related to the formation of blocking high over Alaska (Hayasaka et al. 2016). The warm and dry air masses (286 K) in **Fig. 4(d)** ((4)12Jul.'04-IA) were an exception. From several daily temperature charts before HS peak day (12 July 2004), warm air masses were formed in the east of the Bering Sea and moved to the Gulf of Alaska. Finally, they entered Interior Alaska. **Fig. 4(d)** refers to these warm air masses as mTe (maritime temperate).

Temperature charts of each top HS peak day in NK and SK are shown in **Fig. 5**. Although there are fewer than 3,000 HSs in both places, we found warm and dry air masses (cTe) over both study areas. As **Fig. 5(a)** indicates, we found many fires either in NK or in the vicinity areas of NK under or near cTe (288 K). From **Fig. 5(b)** for SK, many fires were found under cTe (292 K).

From the above 12 temperature charts (**Figs. 1**, **3**, **4**, and **5**), there is a relatively strong correlation between HSs (very active fires) and warm air masses (cTe and mTe) in the four study regions. In addition, from more than 100 daily temperature charts (not shown here), we found that fires tended to become very active as warm air masses from south are reaching and passing each study region. The following sections discuss the relationship between fire activities and warm air masses (or increases of number of HSs toward hotspot peaks of each fire-period) (**Fig. 8**) during each fire-period, and common weather conditions at upper (500 hPa) and lower air (925 hPa).

### *3.2 High-pressure systems during active fire-periods*

The high-pressure systems at upper air will make conditions favorable to fire. They produce warm and dry conditions at near surface level as a result of the inherent downward flow of high-pressure systems (University Corporation of Atmospheric Research, 2009). High-pressure systems are readily apparent during each fire-period. **Fig. 6** shows two average weather maps at upper air (500 hPa) during active fire-periods for SS and IA. From average weather maps, stagnant and persistent weather conditions are easily visible.

In Sakha, a ridge shown by a dotted line in **Fig. 6(a)** is made by large westerly meandering. This is due to stagnant low-pressure systems located in western Siberia ($L_{5480}$, 64 N 60 E). This ridge and the temperature ridge in **Fig. 1** were almost overlapped.

In Alaska, persistent high-pressure systems in the southeast ($H_{5760}$, 62 N 150 W) are also generated by the large meandering westerlies over the Bering Sea. A ridge along the west coast line of North America is found in **Fig. 6(b)**. This ridge and the temperature ridge in **Fig. 4 (a)** were almost overlapped. Other high- and low-pressure systems in Alaska during fire-periods are reported in Hayasaka et al., 2016.

In **Fig. 6**, we could see a few cutoff lows and troughs. The trough over the Bering Sea in **Fig. 6(a)** is suggesting cool and wet conditions for IA. On the other hand, the trough over the Bering Sea in **Fig. 6(b)** is also suggesting cool and wet conditions for SS and NK. These weather conditions, high- and low-pressure systems over four study regions could partially explain about different trend of fire years in SS and IA (**Fig. 2**, section 2.4). As seen in **Fig. 2**, active fires in SS and IA from 2002 to 2017 did not occur in the same year. These trends of fire year will be discussed by considering the scale and flow characteristics of the large meandering westerlies.

We attempted to clarify the relationship between high-pressure systems and warm air mass. In **Fig. 4(a)**, Sakha region had warm and dry air masses (cTe 284 K, 66 N 132 E) in a rectangle with a dotted line and a ridge at upper air (500 hPa) formed over Sakha on August 14, 2005 (weather maps not shown here). But ridge or high-pressure systems over Sakha did not last long. As a result, fires could not become active (see small number of red dots in SS in **Fig. 4(a)**). This means persistent high-pressure systems at upper air are a necessary condition for active fires in addition to warm air mass. In other words, the presence of warm air mass alone will not cause active fires. “Persistent” high-pressure systems at upper air are inherently making warm and dry conditions or the requirement conditions for large-scale fires.

### *3.3 Wind conditions during active fire-periods*

Satellite imagery in **Fig. 1** shows the fire situation on August 19, 2002 (HS peak day of the top fire-period, “(1)19Aug.'02-SS” in Sakha. The maximum number of HSs was 8,796 and fires mainly occurred in the western half of the study region (SS). Smoke from active fires clearly show wind direction was almost southeasterly. **Fig. 7** shows the lower-level weather map (925 hPa) on 19 August 2002.

In Alaska, drastic wind direction change occurred during a few active fire-periods related to Rossby wave breaking (RWB, **Table 1**). Fires became very active firstly from south and southwesterly wind. After that, fires were more active under strong northeast and easterly wind from the Beaufort Sea High (Hayasaka et al., 2016). From these results, we could not clearly show wind direction effect on active fires or relationship between wind direction and fires.

The large pressure gradient over the fire region in **Fig. 7** suggests relatively high wind velocity. In addition, from many weather maps of lower air during each fire-period, we noticed the height difference in active fire regions becomes more prominent as warm and dry air masses move from south to north. Therefore, we carried out a preliminary wind analysis to explain one of the reasons for the rapid increase of daily HSs related to northward movement of warm and dry air masses. Hayasaka et al. (2016) and (2019) evaluate the effect of wind velocity on fire activities in Alaska and Southern Sakha respectively. But those wind analysis were primitive analysis and carried out using pressure gradient between two fixed positions. Here, we use wind velocity and wind direction from U- and V- distribution maps at lower air (925 hPa) (Kalnay et al., 1996).

To evaluate the effect of wind velocity on widespread and concurrent fires in SS, wind velocity ($V_f$) at wind observation point ("x" mark in **Figs. 1**, **3**, and **7**) is introduced for preliminary wind analysis. $V_f$ is obtained from wind velocities of u and v from the U- and V- distribution map. Daily changes of $V_f$ and wind direction during the top fire-period ((1)19Aug.'02-SS) are shown in **Fig. 8**.

From **Fig. 8**, relatively high wind velocity of more than 8 m/s was observed on 15 and 19 August. These velocities could make first and second HSs peak (**Fig. 8**). In addition, wind directions were almost constant as SE (southeasterly wind) from August 12 (first day) until August 23. Therefore, fires became active under relatively fast wind velocity with constant wind direction.

To clarify the relationship between fires, the (HSs) and wind velocity, regression equation is calculated:

$$NH_S=1190.3+106.55V_f+89.643V_f^2 \quad (R^2=0.79347) \qquad (1)$$

where $NH_S$ is Number of HSs, $V_f$ is wind velocity (m/s) at wind observation point (60 N 125 E, 925 hPa).

Errors in number of HSs varied from -41 % (August 20) to 27 % (August 17) except on the last day (August 25, error: 370 %). The relatively high value of decision coefficient ($R^2$=0.79) suggests that most fires became active mainly due to wind velocity.

The remaining fire-periods in SS (from the second- to the fifth-most-active fire-periods for SS in **Table 2**) had strong wind conditions. These occurred under various weather patterns formed by a combination of low- and high-pressure systems, ridges and troughs (not shown here). Thus, it was difficult to demonstrate a common lower-level weather pattern during active fire-periods. However, as a first step, we apply **Eq. (1)** to estimate fire activity on the peak HS day of each fire-period. Each $V_f$ for **Eq. (1)** is obtained at each wind observation point (see "x" mark in **Fig. 3**).

Errors in HSs were -20, -24, -34 and 25 % from the second- to the fifth-most-active fire-periods. These results suggest that wind conditions will explain fire activities of other top fire-periods. The above high value of decision coefficient ($R^2$=0.79) in Eq. (1) also suggests that wind velocity is one of the most important factors for other study regions, especially IA where strong wind from the Beaufort Sea High observed (Hayasaka et al., 2016).

In sum, we showed that fires in Southern Sakha (SS) are activated under a relatively high wind velocity with the same wind direction. These wind conditions occurred when warm and dry air masses (cTe) were approaching, stagnating, and passing over Southern Sakha (SS) (**Figs. 1, 3** and **8**).

## 4. Conclusions

We examined the relationship between active fires (hotspots) and warm and dry air masses, and related common weather conditions by analyzing many weather maps, and temperature charts and wind velocity maps during active fire-periods. Results permitted the following conclusions:

1. Very active fires (large number of HSs) during the top 13 fire-periods occurred when warm and dry air masses from the south were approaching, stagnating, and passing each study region (**Figs. 1** & **3** for SS, **Fig. 4** for IA, and **Fig. 5** for NK & SK).
2. Movements of warm and dry air masses from south to study regions were not significantly affected by weather conditions at lower air. Their movements were mostly related to high-pressure systems at upper air (**Fig. 6(a)** and **Fig. 1** for IA**, Fig. 6(b)** and **Fig. 4 (a)** for SS). As movements of warm and dry air masses can be easily visualized by making a daily temperature chart, we could forecast active fires just before a few days with high probability (For example, first HS peak in **Fig. 8** occurred on Aug. 15, three days after active fires started on Aug. 12). This approach will be useful for future fire forecasts.
3. The top six HS peaks (very active fires) in SS were well correlated with strong wind velocities obtained from preliminary wind analysis at lower air (**Figs. 7 & 8)**. This dependence of fires on wind velocity is common to both SS and IA (Hayasaka et al., 2016). This suggests wind velocity is a crucial parameter for very active fires in addition to dry and warm conditions.
4. At upper air (500 hPa), averaged weather maps (**Fig. 6**) during active fire-periods clearly showed the large westerlies meandering due to stagnating low-pressure systems, as well as formation of persistent high-pressure systems over active fire regions. Most active fire-periods (**Table. 2**) occurred under persistent high-pressure systems that will make fire favorable conditions or warm and dry near surface level.
5. SS and IA are fire prone regions compared with NK and SK (**Fig. 2** and **Tables 1 & 2**). This difference in fire activity suggests we should discuss fire regimes including landscape (terrain) of each study regions in future.

We do hope this study will help improve fire forecast in boreal forests, and also lead to mitigation against climate change by reducing active forest fires.

## Acknowledgements

This research was partially supported by the Center for International Forestry Research (CIFOR) with funding by the Government of Japan. This study was carried out under the Joint Research Program of the Japan Arctic Research Center. We would like to thank to "The NCEP/NCAR 40-Year Reanalysis Project". We acknowledge the use of data and imagery from LANCE FIRMS operated by NASA's Earth Science Data and Information System (ESDIS) with funding provided by NASA Headquarters.

## References


Abatzoglou, J. T. and Crystal, A. K. (2011). Relative importance of weather & climate on wildfire growth in interior Alaska. Int. J. of Wildland Fire, 20, 479–486.

Balzter, H., Gerard, F.F., George, C.T., Rowland, C.S., McCallum, I., Jupp, T.E., Shvidenko, A., Nilsson, S., Sukhinin, A., Onuchin, A., Schmullius, C., 2005. Impact of the Arctic Oscillation pattern on interannual forest fire variability in Central Siberia. Geophys. Res. Lett., 32, L14709, doi:10.1029/ 2005GL022526.

Bell, G. (2004). Special Climate Summary, April-July 2004, Hot in Alaska, Cool over Central North America, Wet in South-Central U.S., Accessed 27 Oct. 2015. http://www.cpc.ncep.noaa.gov/products/ expert_assessment/alaska.pdf

Calef, M. P., McGuire, A. D., Epstein, H. E., Rupp, T. S., Shugart, H. H. (2005). Analysis of vegetation distribution in interior Alaska and sensitivity to climate change using a logistic regression approach. Journal of Biogeography, 32, 863-878. https://onlinelibrary.wiley.com/doi/full/10.1111/j.1365-2699.2004.01185.x

Fauria, M., & Johnson, E. A. (2006). Large-scale climatic patterns control large lightning fire occurrence in Canada and Alaska forest regions. J. Geophys. Res., 111, G04008, 2006. doi:10.1029/2006JG000181.

Fauria, M., & Johnson, E. A. (2008). Climate & wildfires in the North American boreal forest. Phil., Trans. R. Soc. B 363, pp. 2317–2329, 2008. doi:10.1098/rstb.2007.2202.

Field,R.D., Spessa, A.C., Aziz, N.A., Camia, A., Cantin, A., Carr,R., Groot,W. J. de, Dowdy,A.J., Flannigan, M.D., Manomaiphiboon,K., Pappenberger,F., Tanpipat,V., and Wang, X., Development of a Global Fire Weather Database, Nat. Hazards Earth Syst. Sci., 15, pp. 1407–1423, 2015.

Forkel, M., Thonicke, K., Beer, C., Cramer,W., Bartalev, S., Schmullius, C., 2012. Extreme fire events are related to previous-year surface moisture conditions in permafrost underlain larch forests of Siberia. Environ. Res. Lett. 7 (4), 044021.

Giglio, L., Csiszar, I., Justice, C. O. (2006). Global Distribution and Seasonality of Active Fires as Observed with the Terra and Aqua Moderate Resolution Imaging Spectroradiometer (MODIS) Sensors. Journal of Geophysical Research, 111, doi:10.1029/2005JG000142

Gillett, N.P., Weaver, A.J., Zwiers, F.W., and Flannigan, M.D., 2004. Detecting the effect of climate change on Canadian forest fires. Geophys. Res. Lett., 2004, vol. 31, 18211. Doi 10.1029/2004GL020876

Hayasaka. H., 2007. Recent Large Scale Fires in Boreal and Tropical Forests, Journal of Disaster Research, 2-4, 265-275.

Hayasaka. H., 2011. Recent Vegetation Fire Incidence in Russia, Global Environmental Research, AIRIES, 15-1, 5-13, 2011.

Hayasaka. H., Tanaka H. L., Bieniek, P. A., 2016. Synoptic-scale fire weather conditions in Alaska, Volume 10, Issue 3, Polar Science, pp 217-226. http://dx.doi.org/10.1016/j.polar.2016.05.001

Hayasaka. H., Yamazaki, K., Naito, D., 2019. Weather Conditions and Warm Air Masses in Southern Sakha during Active Wildfire Periods, J. Disaster Res., 14-4, pp. 641-648.

Onuchin, A., Shvidenko, A., Pavlov, I. and Schepaschenko, D. (2007). RUSSIAN FORESTS: IMPACTS ON EARTH SYSTEM, Conference: XIII World Forestry CongressAt: Buenos Aires, ArgentinaVolume: pp. 18-25, available at: https://www.researchgate.net/publication/266342817 (last access: 2 Jan. 2019).

Ponomarev, E. I., Kharuk, V. I., Ranson, K.J., 2016. Wildfires Dynamics in Siberian Larch Forests, Forests 2016, 7, 125; doi:10.3390/f7060125 www.mdpi.com/journal/forests

IPCC, 2013. Climate Change 2013: The Physical Science Basis. Contribution of Working Group I to the Fifth Assessment Report of the Intergovernmental Panel on Climate Change. Stocker, T.F., Qin, D., Plattner, G.-K., Tignor, M., Allen, S.K., Boschung, J., Nauels, A., Xia, Y., Bex, V., and Midgley, P.M., Eds., Cambridge: Cambridge University Press, 2013. http://www.ipcc.ch/report/ar5/wg1/, Latest access 2018 Jan.21.

IPCC, 2016. Climate Change 2014: Impacts, Adaptation, and Vulnerability. Summaries, Frequently Asked Questions, and Cross-Chapter Boxes. In C.B. Field, Contribution of Working. Group II to the Fifth Assessment Report of the Intergovernmental Panel on Climate Change, Geneva: World Meteorological Organization.

Kalnay E., Kanamitsu, M., Kistler R., Collins, W., Deaven, D., Gandin, L., Iredell, M., Saha, S., White, G., Woollen, J., Zhu, Y., Chelliah, M., Ebisuzaki W., Higgins, W., Janowiak, J., Mo, K. C., Ropelewski, C., Wang J., Leetmaa, A., Reynolds, R., Jenne. R., Joseph, D., 1996. The NCEP/NCAR 40-year reanalysis project. Bull. Amer. Meteor. Soc., 77, 437-470.

Kasischke, E.S., Verbyla, D., Rupp, T.S., McGuire, A.D., Murphy, K.A., Allen, J.L., et al., 2010. Alaska's changing fire regime: Implications for the vulnerability of its boreal forests, Can. J. Forest Res., vol. 40, pp. 1313–1324.

Köppen climate classification, https://www.thoughtco.com/the-worlds-koppen-climates-4109230 (last access: 5 Jun 2019).

Lenton, T.M., Held, H., Kriegler, E., Hall, J.W., Lucht, W., Rahmstorf, S., Schellnhuber, H.J., 2008. Tipping elements in the Earth's climate system. Proc. Natl. Acad. Sci. 105 (6), 1786–1793.

McGuire, A. D., F. S. Chapin, III, J. E. Walsh, and C. Wirth. 2006. Integrated regional changes in arctic climate feedbacks: implications for the global climate system. Annual Review Environment and Resources 31:61–91.

Schaphoff, S., Reyer, C. P. O., Schepaschenko, D., Gerten, D. Shvidenko, A., 2015. Tamm Review: Observed and projected climate change impacts on Russia's forests and its carbon balance. Forest Ecol. Manage. , http://dx.doi.org/10.1016/j.foreco.2015.11.043

Shahgedanova., M. (2003), Climate at Present and in the Historical Past, In M. Shahgedanova (Ed.), The Physical Geography of Northern Eurasia (70-102), Oxford, United Kingdom: Oxford University Press, http://www.rusnature.info/geo/03_2.htm

Skinner, W. R., Stocks, B. J., Martell, D. L., Bonsal, B., & Shabbar, A. (1999). The association between circulation anomalies in the mid-troposphere and area burned by wildland fire in Canada. Theor. Appl. Climatol. 63, 89–105, doi:10.1007/s007040050095

Skinner, W. R., Flannigan, M. D., Stocks, B. J., Martell, D. L., Wotton, B. M., Todd, J. B. Mason, J. A., Logan, K. A., & Bosch. E. M., (2002). A 500 hPa synoptic wildland climatology for large Canadian forest fires 1959–1996. Theor. Appl. Climatol. 71 157–69, 2002.

Tanaka, H. L., Watarai, Y., Kanda, T., 2004. Energy spectrum proportional to the squared phase speed of Rossby modes in the general circulation of the atmosphere. Geophys. Res. Lett. 31 (13), 13109,. http://dx.doi.org/10.1029/2004GL019826.

Tchebakova, N. M., Parfenova, E., Soja, A. J., 2009. The effects of climate, permafrost and fire on vegetation change in Siberia in a changing climate. Environmental Research Letters, Volume 4, Number 4.

Valendik E. N., 1996. Temporal and Spatial Distribution of Forest Fires in Siberia. Fire in Ecosystems of Boreal Eurasia, Goldammer J. G., Furyaev. V. V. (ed). Kluwer Academic Publishers: Dordrecht; 129-138.

Wendler, G., Conner, J., Moore, B., Shulski, M., & M. Stuefer. (2011). Climatology of Alaskan wildfires with special emphasis on the extreme year of 2004. Theoretical and Applied Climatology, 104(3-4), 459–472.

# Figures and Tables with Legends

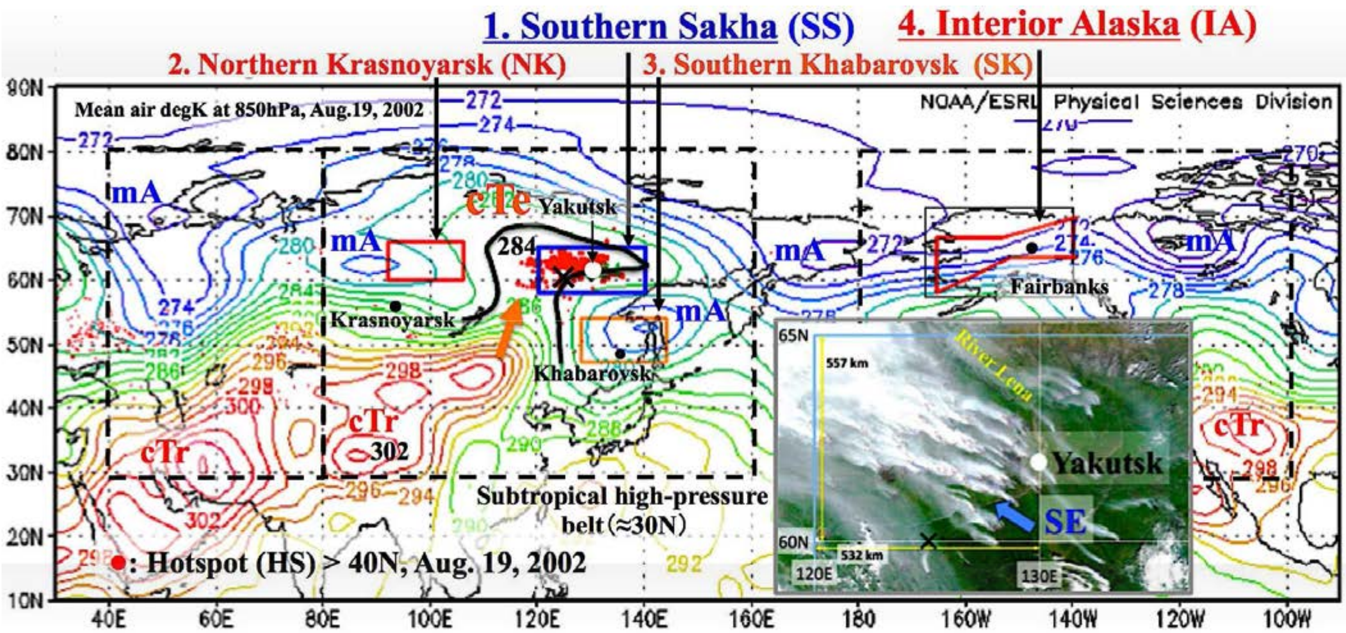


Fig. 1. Map of four study regions in boreal regions on the temperature chart (850 hPa) on 19 August 2002. Four study regions: 1. Southern Sakha (SS), 2. Northern Krasnoyarsk (NK), 3. Southern Khabarovsk (SK), and 4. Interior Alaska (IA)) in boreal regions. cTe: continental temperate, mA: maritime arctic and cTr: continental tropical (Shahgedanova, 2003). Temperature contour line (284 K) near Southern Sakha (SS) is thickened to show location and shape of cTe. Arrowhead orange color line shows approximate northward routes of cTe from south to SS (Hayasaka et al. 2019). Inserted satellite image was captured on August 19, 2002 during the top fire-period in SS. Image shows the most active concurrent widespread forest fires in SS under southeasterly wind. Image file name is Russia.A2002231.0300.250m from MODIS (Most old MODIS images, including this image, are not available due to data disk failure). Each line of latitude, longitude and the study area (blue line) in satellite image are drawn in approximate positions and are not accurate. Major cities related to four study regions are shown by a black or white solid circle (●,○). Hotspots (fires) are drawn by a red solid circle (●) and most hotspot are drawn in large size especially in study regions. Hotspots in red color are plotted on the weather map using computer-aided design (CAD) software (Vector-Works ver. 2010 SP4). "X" mark is wind (velocity and direction) observation point (60 N 125 E) for wind velocity analysis in section 3.3. Rectangles with dotted lines show cover areas and are used commonly in Figs. 3, 4 and 5.

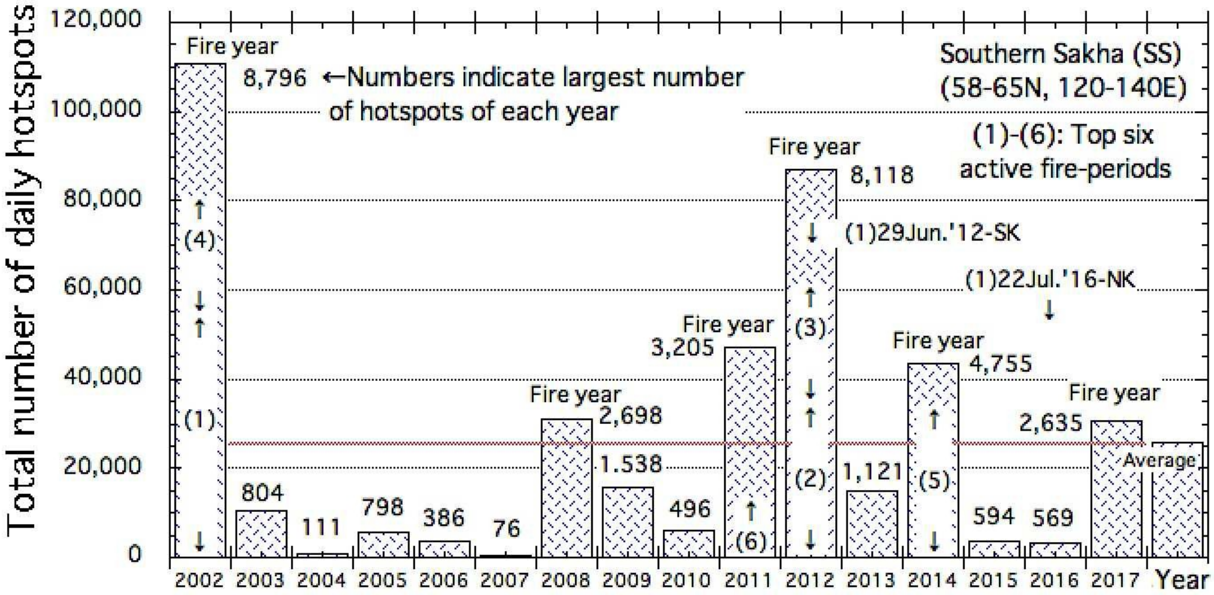


(a) Fire history in Southern Sakha (SS), Southern Khabarovsk (SK), and Northern Krasnoyarsk (NK). Top six active fire-periods ((1)-(6)) in SS are embedded in corresponding annual bar graphs. Top active fire-periods in SK and NK are shown by "↓" with active fire-period name (1)29Jun.'12-SK and (1)22Jul.'16-NK. Numbers near each bar graph indicate largest number of hotspots of each year. Numbers near each bar graph show largest number of HSs of each year.

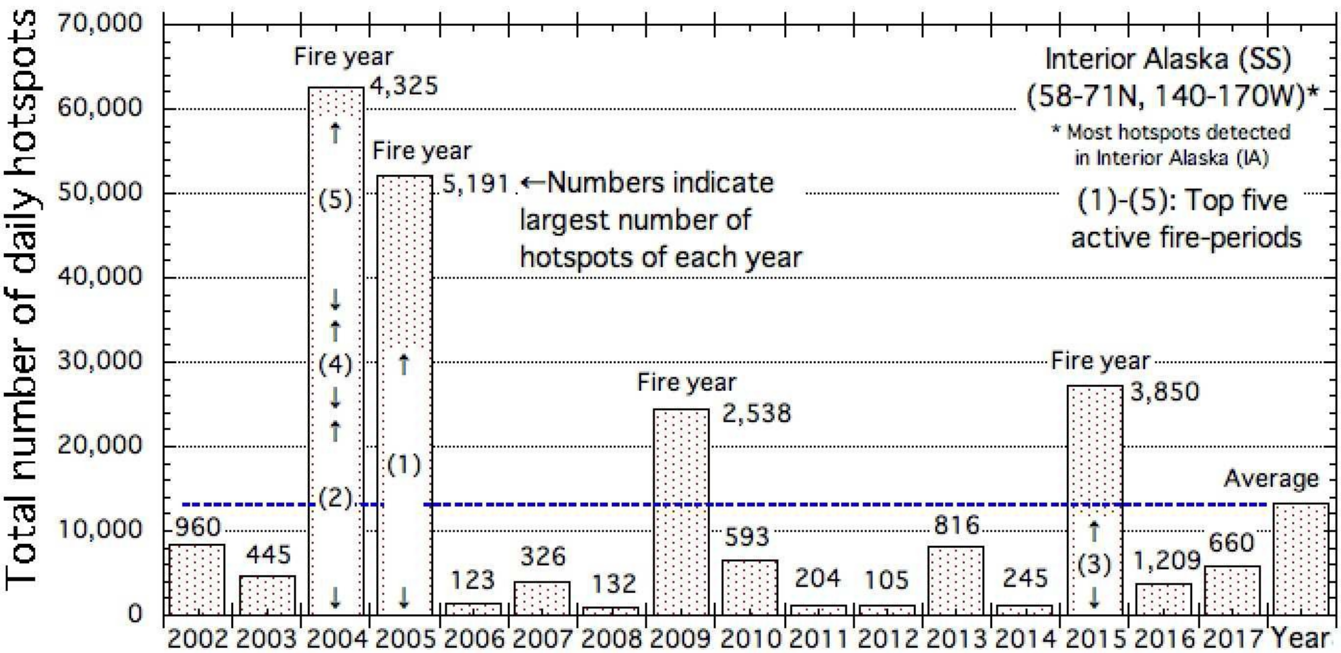


**(b)** Fire history in Alaska (IA). Top five active fire-periods ((1)-(5)) are embedded in corresponding annual bar graphs. See captions for **Fig. 2 (a)**

**Fig. 2.** Annual total number of hotspots (HS) from 2002 to 2017.

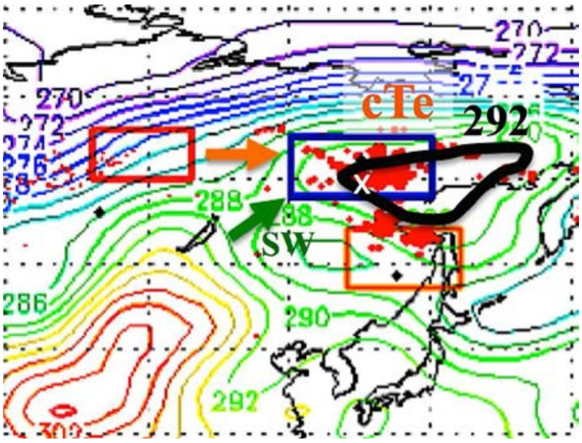


**(a)** (2)3Aug.'12-SS (HS=8,118), cTe=292 from West, Southwesterly Wind (X:60N 130E)

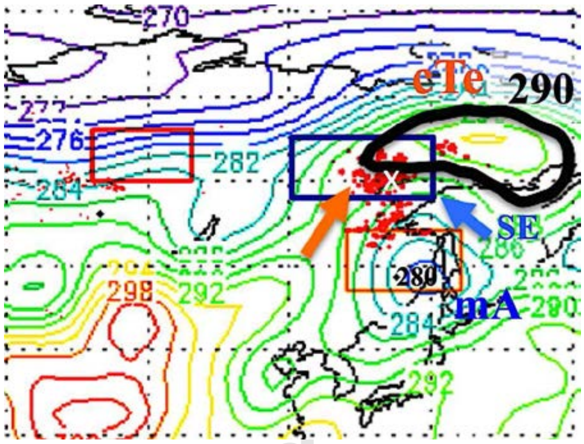


**(b)** (3)14Jul.'12-SS (HS=5,829) , cTe=290 from Southwest, Southeasterly Wind (X:60N 135E)

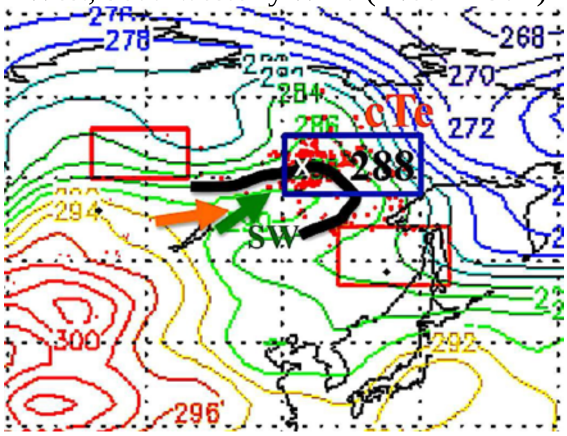


**(c)** (4)20Jul.'02-SS (HS=5,270) , cTe=292 from West, Southwesterly Wind (X:62N 122E)

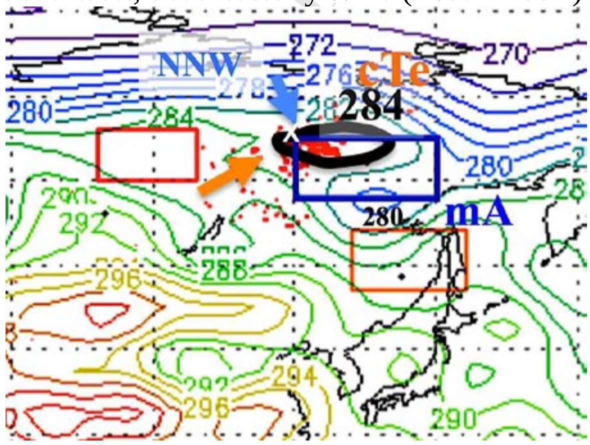


**(d)** (5)22Jul.'14-SS (HS=4,775) , cTe=284 from West, North-northwesterly Wind (X:66N 118E)

**Fig. 3.** Temperature chart on each top HS peak day in SS (Southern Sakha). See captions for **Fig. 1**. Latitude and longitude lines are the same as those in **Fig. 1**.

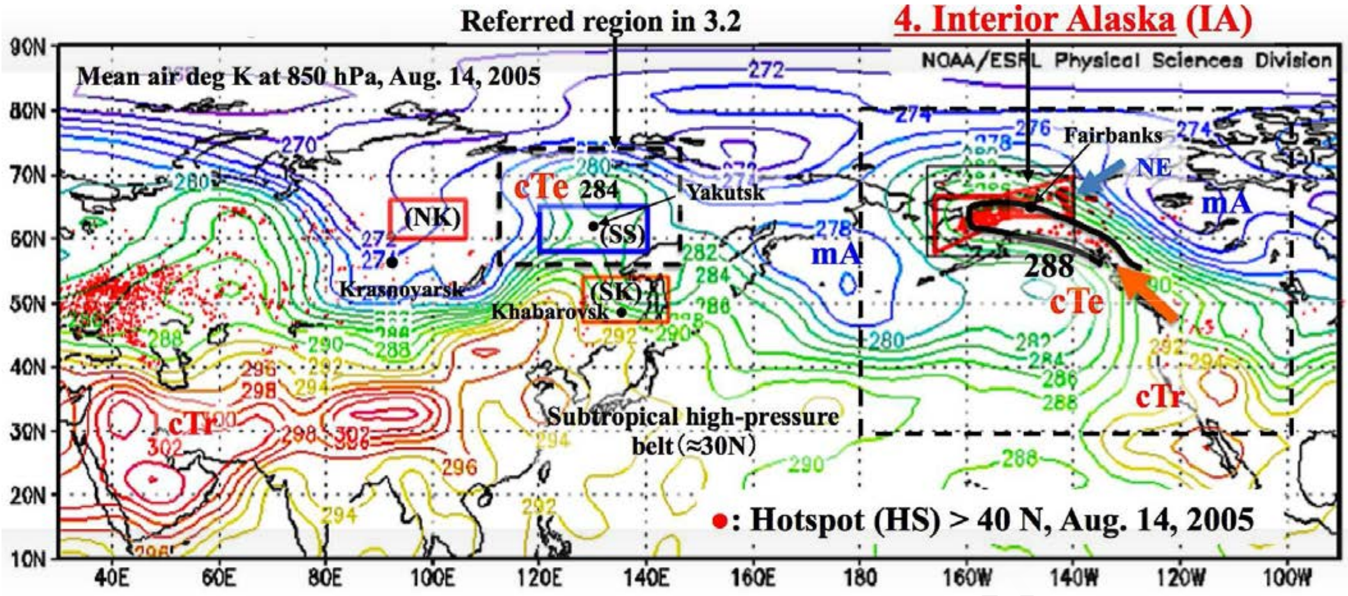


**(a)** (1)14Aug.'05-IA, (HS=5,191), cTe=288 from Southeast, Northeasterly Wind. A dotted line rectangle near SS is referred region in **3.2** and shows warm and dry air masses (cTe, 284 K) passing Southern Sakha region.

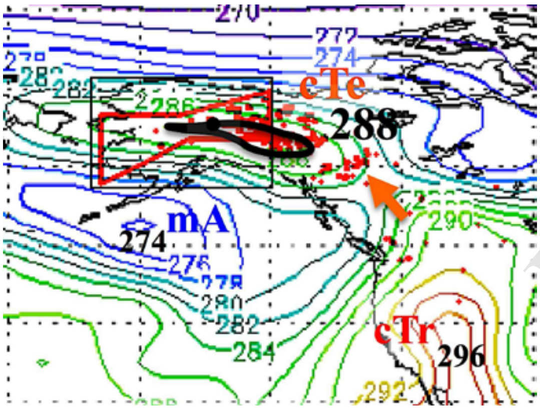


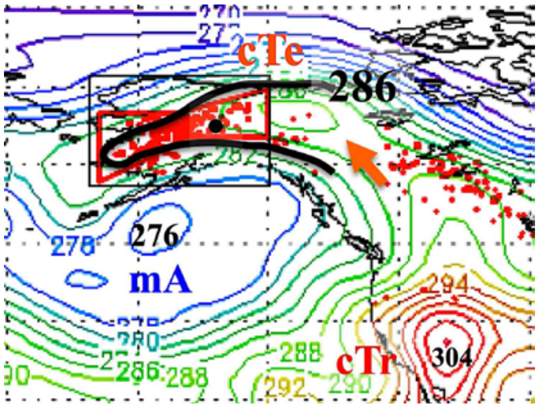


**(b)** (2)29Jun.'04-IA (HS=4,325), cTe=288 from Southeast, Easterly Wind.

**(c)** (3)25Jun.'15-IA (HS=3,850), cTe=286 from Southeast, Southwesterly Wind.

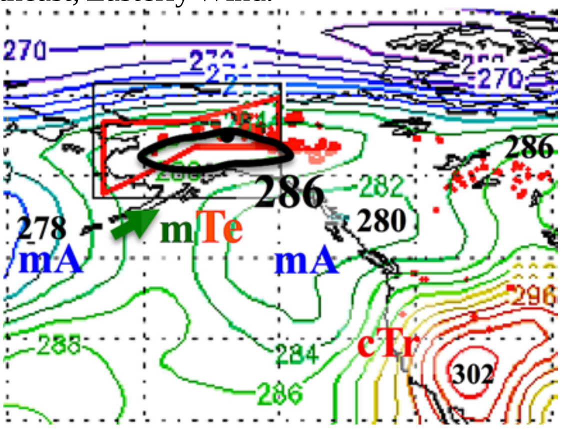


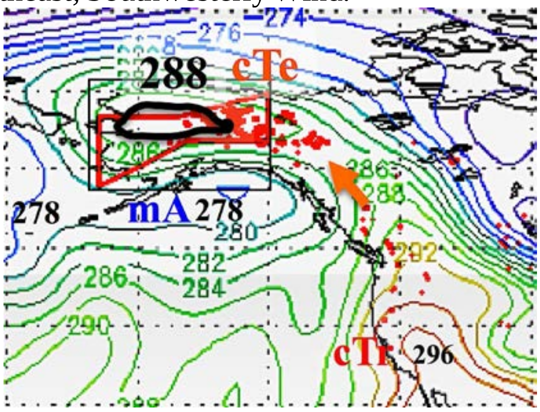


**(d)** (4)12Jul.'04-IA (HS=3,521), mTe=286 from Southwest, Southeasterly Wind.

**(e)** (5)20Aug.'04-IA (HS=3,053), cTe=288 from Southeast, Easterly Wind.

**Fig. 4.** Temperature chart on each top HS peak day in IA (Interior Alaska). See captions for **Fig. 1**. Latitude and longitude lines are the same as those in **Figs. 1** and **4(a)**.

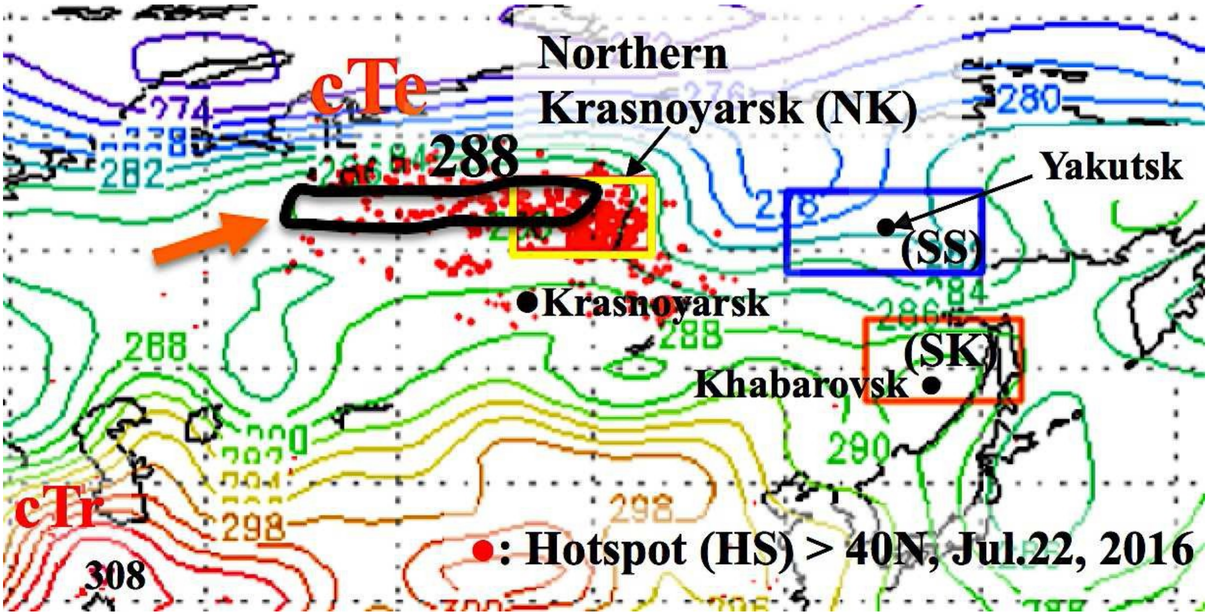


**(a)** (1)22Jul.'16-NK (HS=2,198), cTe=288 from Southwest, Northwesterly Wind.

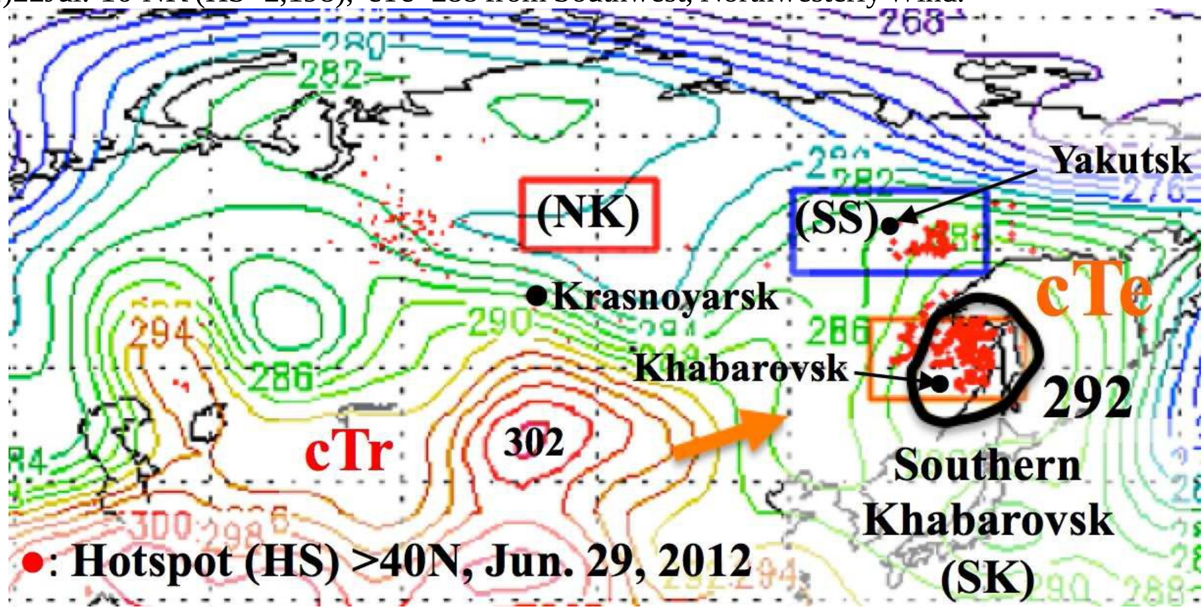


**(b)** (1)29Jun.'12-SK (HS=2,683), cTe=292 from Southwest, Southwesterly Wind.

**Fig. 5.** Temperature chart on each top HS peak day in Northern Krasnoyarsk (NK) and Southern Khabarovsk (SK). See captions for **Fig. 1**. Latitude and longitude lines are the same as those in **Fig. 1**.

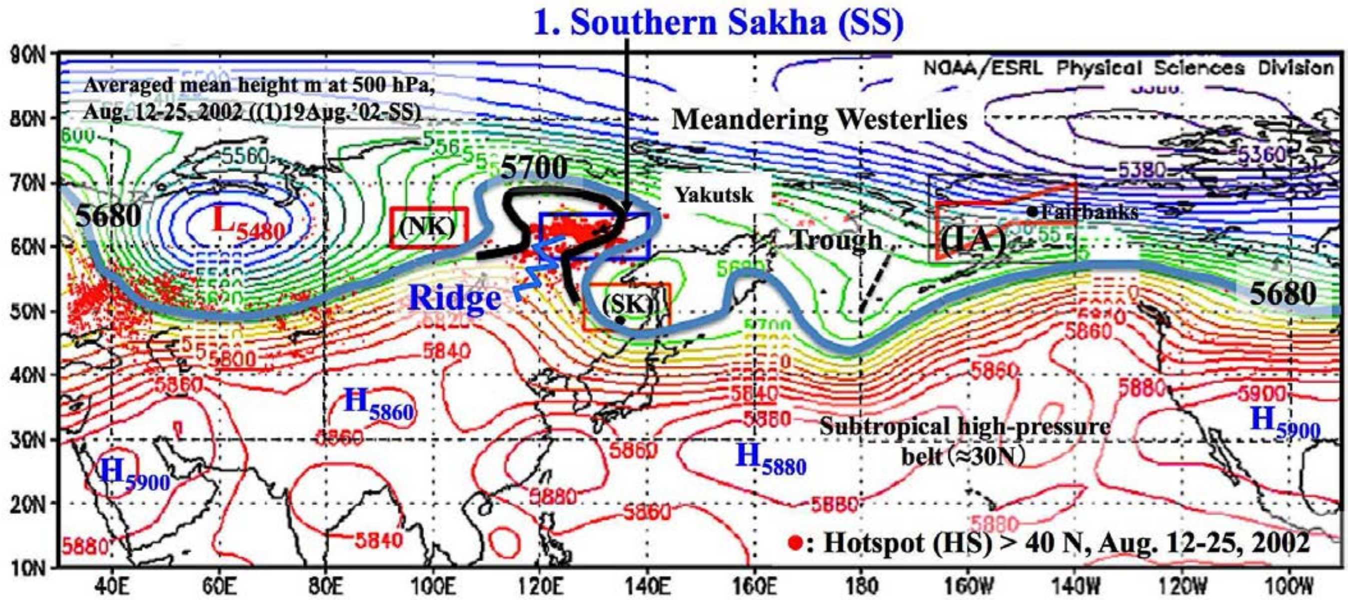


**(a)** Large meandering westerlies during top fire-period in SS ((1)19Aug.'02-SS), "H" and "L" stand for high- and low-pressure system. Subscripts of each "H" and "L" mean the highest height (m) of high- pressure system and the lowest height (m) of low-pressure system respectively.

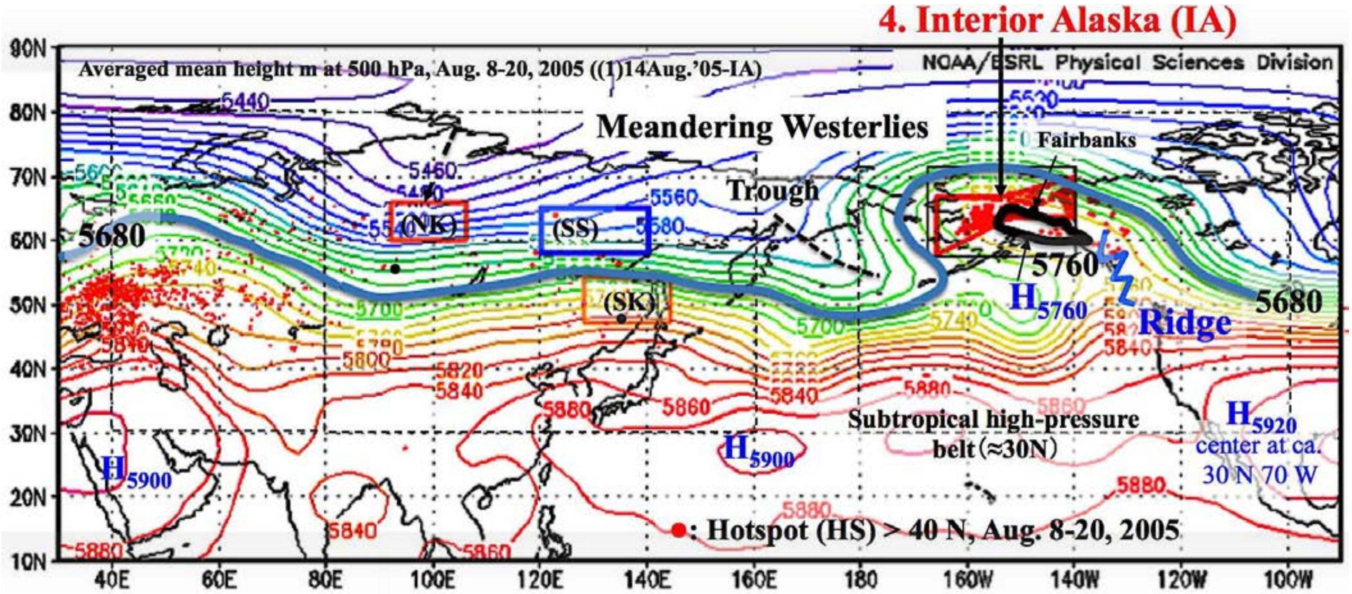


**(b)** Large meandering westerlies during top fire-period in IA ((1)14Aug.'05-IA), see captions for **(a)**

**Fig. 6**. Averaged weather maps at upper air (500 hPa). The isoline (5,680 m) is thickened to evaluate meandering westerlies.

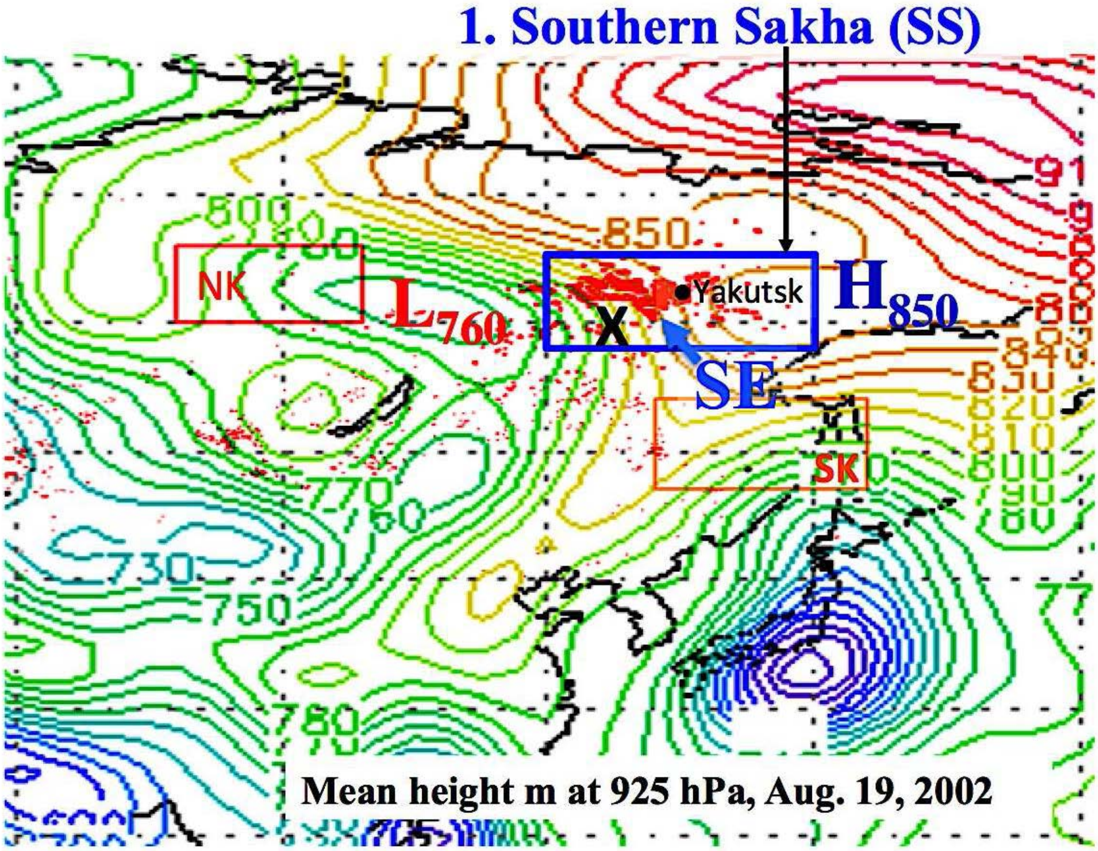


**Fig. 7.** Weather map (925 hPa) on August 19, 2002 ((1)19Aug.’02-SS)). See captions for **Fig. 1**. Latitude and longitude lines are the same as those in **Fig. 1 .**

**Fig. 8.** Wind velocity and direction, and hotspots (the top fire-period ((1)19Aug.'02-SS). Wind velocity ($V_f$) at wind observation point (see "x" mark in **Fig. 1**).

**(Table)**

**Table 1**

Four study regions: * Area for polygon shape shown in **Fig. 1,** ** Area ratio of each region when the area of SS is set to 1, *** Köppen climate classification (D (Continental), first subscript: f (Without dry season), w (Dry winter), and second subscript: a (Hot summer), b (Warm summer), c (Cold summer), and d (Very cold winter))

| Study region | Latitude | Longitude | Area ($x10^3$ $km^2$) | Area ratio** | Climate type*** | Temp. in July (D, ave. high & low) | Rainfall in July (mm) | Weather station |
|---|---|---|---|---|---|---|---|---|
| SS | 58-65 N | 120-140 E | 840 | 1.00 | Dfd,Dwd | 25.5-12.7 | 39 | Yakutsk |
| NK | 60-66 N | 92-106 E | 469 | 0.56 | Dfc | 24.8-13.4 | 76 | Krasnoyarsk (south of NK) |
| SK | 47-54 N | 128-144 E | 879 | 1.05 | Dfa,Dwb | 26.6-16.8 | 133 | Khabarovsk |
| IA | 60-69 N | 140-166 W | 681* | 0.81 | Dfc | 22.6-11.3 | 55 | Fairbanks |

**Table 2**

The top 11 active fire-periods in Southern Sakha (SS) and Interior Alaska (IA)

* The top six fire-periods in SS are shown in the top and the top five fire-periods in IA are listed in the bottom, ** Fire period related to Rossby wave breaking (RWB)

| Fire-period (rank, day, month, year, region) * | Largest daily num. of HS | Total num. of HS | Num. of fire days (fire-period) |
|---|---|---|---|
| (1)19Aug.'02-SS | 8,796 | 57,033 | 15(Aug.11-25) |
| (2)3Aug.'12-SS | 8,118 | 35,254 | 12(Jul.25-Aug.5) |
| (3)14Jul.'12-SS | 5,829 | 29,756 | 10(Jul.7-16) |
| (4)20Jul.'02-SS | 5,270 | 23,752 | 12(Jul.14-25) |
| (5)22Jul.'14-SS | 4,755 | 36,002 | 22(Jul.14-Aug.4) |
| (6)17Jul.'11-SS | 3,205 | 14,871 | 11(Jul.12-22) |
| (1)14Aug.'05-IA** | 5,191 | 30,886 | 13(Aug.8-20) |
| (2)29Jun.'04-IA** | 4,325 | 22,148 | 16(Jun.18-Jul.3) |
| (3)25Jun.'15-IA | 3,850 | 12,710 | 8(Jun.19-Jun.26) |
| (4)12Jul.'04-IA | 3,521 | 12,464 | 9(Jul.10-18) |
| (5)20Aug.'04-IA** | 3,053 | 23,394 | 24(Aug.6-29) |